

Electronic transport in doped amorphous silicon

J. Kakalios and R. A. Street

Xerox Palo Alto Research Center, Palo Alto, California 94304

(Received 16 June 1986)

The temperature dependence of the dc dark conductivity of doped hydrogenated amorphous silicon is explained by the defect-compensation model of doping with the proposal that the structure is in metastable thermal equilibrium. Observed conductivity activation energies and preexponential factors can be accounted for quantitatively. When the localized state distribution is in thermal equilibrium, the conductivity preexponential factor is the Mott minimum metallic conductivity.

Since the discovery in 1975 by Spear and LeComber that hydrogenated amorphous silicon (a -Si:H) could be doped,¹ there has been a rapid increase in our understanding of transport in amorphous semiconductors. It is therefore surprising that basic questions persist regarding the temperature dependence and magnitude of the dc conductivity.^{2,3} Even when the distinction between bulk and surface conduction is made and measurements are performed which minimize space-charge effects, many puzzles exist. Arrhenius plots of the temperature dependence of the dc dark conductivity exhibit an upward kink at high temperature ($T \geq 400$ K). The various models to explain the kink include two separate transport paths, potential fluctuations, and shifts of the conduction-band edge with temperature.³⁻⁵ Also, no agreed explanation exists for the Meyer-Neldel rule, an observed exponential increase of the conductivity prefactor with activation energy.³ Finally, the connection between the preexponential factor σ_0 and the minimum metallic conductivity remains a subject of controversy.⁶ In this Rapid Communication we will show that Street's defect-compensation model of doping,⁷ together with the proposal that the structure of doped a -Si:H is in metastable thermal equilibrium,⁸ can successfully answer these questions.

The temperature dependence of the dc dark conductivity in a -Si:H for conduction above a well-defined mobility edge at energy E_C , is assumed to be³

$$\sigma = \sigma_{\min} \exp[-(E_C - E_F)/kT], \quad (1)$$

where E_F is the Fermi-level energy and σ_{\min} is the minimum metallic conductivity. $E_C - E_F$ may be temperature dependent because of the following: (1) E_F is temperature dependent due to a nonsymmetric distribution of states about E_F (a statistical shift), (2) the band gap is temperature dependent, and (3) electron-phonon coupling may cause E_C to move to lower energies as the temperature is raised.⁹ A linear temperature coefficient γ , defined by

$$E_C - E_F = (E_C - E_F)_0 - \gamma T, \quad (2)$$

results in,

$$\sigma = \sigma_0 \exp(E_a/kT), \quad (3)$$

where $E_a = (E_C - E_F)_0$ is the temperature-independent ac-

tivation energy and

$$\sigma_0 = \sigma_{\min} \exp(\gamma/k) \quad (4)$$

is the preexponential factor.

We present here a few new experimental results which we need, in addition to those published earlier, for the discussion presented below. Doped a -Si:H samples of thickness $\sim 1 \mu\text{m}$ were grown via the rf glow-discharge decomposition of silane (SiH_4) and phosphine (PH_3) for n -type doping; or silane and diborane (B_2H_6) for p -type doping, in a deposition reactor described earlier.¹⁰ Before evaporating chrome coplanar electrodes, a 100-Å n^+ layer (1 vol% PH_3 in SiH_4) was plasma deposited on top of the a -Si:H sample (the n^+ layer was omitted for the boron-doped samples). After the electrodes were deposited the n^+ layer in the gap between the contacts was removed by plasma etching. These contacts yielded linear I - V characteristics for applied voltages up to ± 100 V, thereby eliminating the possibility of space-charge effects due to non-Ohmic contacts. It is known that the coplanar dark conductivity of a -Si:H is sensitive to the presence of surface adsorbates¹¹ and is affected by prior light exposures.¹² All conductivity measurements were made after annealing at 450 K for 30 min in an oil-free vacuum after rapidly cooling the samples back to room temperature (cooling rate ≈ 1 - $2^\circ\text{C}/\text{sec}$). The sample is then cooled to below 200 K, and the conductivity is measured as the sample is warmed up to 450 K (heating rate $\approx 3^\circ\text{C}/\text{min}$).

The conductivity of doped a -Si:H is very sensitive to the rate at which the sample is cooled following a high-temperature anneal, as observed by Ast and Brodsky¹³ and Street, Kakalios, and Hayes.⁸ Figure 1 shows Arrhenius plots of the conductivity for n - and p -type a -Si:H. The room-temperature conductivity can vary by a factor of 2 or more as the cooling rate is changed from $1^\circ\text{C}/\text{sec}$ (\bullet data points) to $0.02^\circ\text{C}/\text{sec}$ (\blacktriangle data points). Above a fairly well-defined temperature (≈ 400 K for n -type and 360 K for p -type a -Si:H) the low-temperature conductivity curves merge, becoming independent of thermal history.

The temperature dependence of σ measured as the samples are warmed following rapid cooling (1 - $2^\circ\text{C}/\text{sec}$) after a high-temperature anneal, for a -Si:H doped with 10, 100, and 1000 ppm PH_3 are shown in Fig. 2. These curves obey Eq. (3) with two sets of E_a and σ_0 values over the temperature range 200-450 K. Activated behavior is

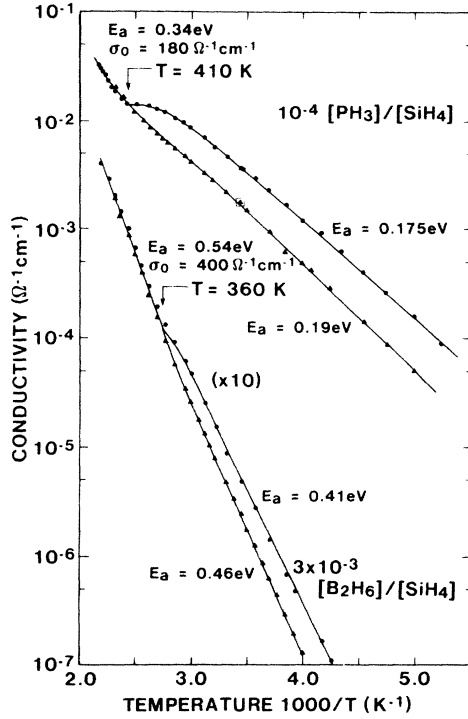


FIG. 1. The temperature dependence of the dc conductivity immediately after annealing for different cooling rates for *n*- and *p*-type doped *a*-Si:H.

observed up to $T \approx 330$ K, with activation energies from 0.21 to 0.16 eV and preexponential factors $\sigma_0 = 5\text{--}10 \Omega^{-1}\text{cm}^{-1}$. Above $T \approx 400$ K Arrhenius behavior is restored, with $E_a \approx 0.3\text{--}0.4$ eV and $\sigma_0 = 200 \Omega^{-1}\text{cm}^{-1}$.

From Figs. 1 and 2, it is clear that the kink in the conductivity and the quench-rate dependence are closely related.

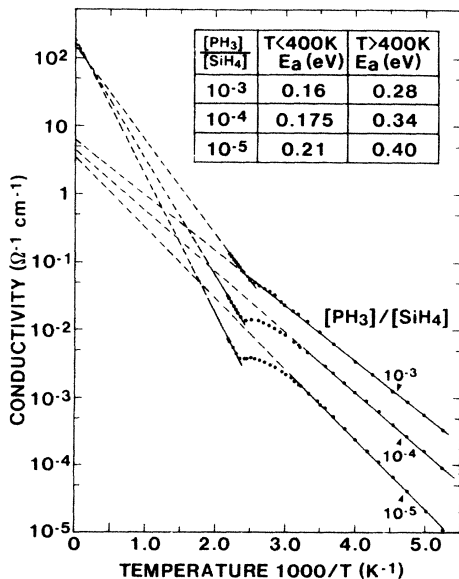
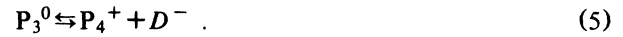


FIG. 2. Conductivity as a function of inverse temperature of *n*-type *a*-Si:H doped with 10, 100, and 1000 ppm phosphine.

ed. We first show that both are a result of thermal equilibration in the sample, based on the defect-compensation model of doping.⁷ According to this model, charged dopant and compensating dangling-bond defect states are in quasithermal equilibrium at the growing surface during deposition. The lowest-energy configuration of doped *a*-Si:H is such that there are approximately equal densities of charged dopants (P_4^+) and compensating dangling-bond states (D^-). For *n*-type *a*-Si:H the doping reaction is thought to be



The Fermi energy E_F is constrained to lie between the charged dangling-bond and dopant states, at an energy we denote E_{min} . It has recently been suggested⁸ that the defect structure, i.e., the densities of P_4^+ and D^- , remain in metastable equilibrium after deposition. The time to reach equilibrium is thermally activated, becoming longer at lower temperatures. In phosphorus-doped *a*-Si:H the equilibration time is of the order of a few seconds near 400 K. Above this temperature the material rapidly comes into thermal equilibrium.

Electrons occupy the shallow band-tail and overlapping donor states. The density n_{BT} of shallow band-tail states is related to the densities of donors (N_{donor}) and dangling bonds (N_{DB}) by the expression

$$n_{BT} \approx N_{donor} - N_{DB} \quad (6)$$

The electron occupancy in the band tail is also defined by

$$n_{BT} = \int_{E_{min}}^{\infty} g(E) [1 + \exp(E - E_F)/kT]^{-1} dE \quad (7)$$

where $g(E)$ is the density of states. During deposition the defect structure is in thermal equilibrium. The Fermi level is therefore at E_{min} , which together with Eq. (7) determines the value of n_{BT} when T is the deposition temperature (typically $\approx 230^\circ\text{C}$).

The model of thermal equilibration allows us to make several qualitative predictions regarding the conductivity temperature dependence. We first address the conductivity below the equilibration temperature. The defect structure is frozen (that is, the time to reach equilibrium is long compared to laboratory time scales), and so the Fermi level is temperature dependent [from Eq. (7)] in order to maintain a constant n_{BT} . Due to the rapidly increasing density of band-tail states, Eq. (7) will be satisfied as the temperature is lowered only if E_F moves away from E_{min} , closer to E_C . We therefore expect the activation energies and prefactors to be strongly influenced by the statistical shift.

On the other hand, above the equilibration temperature the defect structure is in thermal equilibrium. In this case E_F is pinned at the minimum between the P_4^+ and D^- bands at $E_a = E_C - E_{min}$, and there will be no statistical shift. The increase in activation energy above 400 K shown in Figs. 1 and 2 is therefore a natural consequence of the thermal equilibration.

The dependence of n_{BT} (and hence of σ) on cooling rate from above the equilibration temperature has been reported earlier⁸ and is a direct consequence of a metastable defect structure. As the defect structure comes into equili-

brium, the density of donors and dangling bonds changes so as to lower n_{BT} . As shown in Fig. 1 for a 100-ppm PH_3 -doped a -Si:H sample, a large hysteresis is seen upon slow cooling ($\approx 0.02^\circ\text{C}/\text{sec}$) from 450 K, as expected from the thermal equilibration model. The higher activation energy and lower σ_0 of the lower curve (\blacktriangle data points in Fig. 1) reflects the lower n_{BT} obtained by slow cooling. After slow cooling to 330 K the sample was cooled to 200 K and then warmed up to 360 K and then rapidly cooled ($\approx 1^\circ\text{C}/\text{sec}$) to 290 K (boxed data point in Fig. 1). This data point lies on the slow cooling curve, indicating that the defect structure remained fixed up to 360 K.

Our model defines two temperature regimes separated by the equilibration temperature. The kink originates because the statistical shift is present at low temperature but absent at high temperatures. We now show that the model gives quantitative agreement with the data, based on the density of states $g(E)$, shown in Fig. 3. This $g(E)$ is derived from experiment as described elsewhere.¹⁴ The temperature dependence of σ for the low-temperature regime is calculated by numerically integrating Eq. (7), using this density of states and assuming that the structure freezes at 130°C , with E_F at E_{\min} . For a doping level of 10^{-5} we find $E_a = 0.23$ eV and $\sigma_0 = 15 \Omega^{-1}\text{cm}^{-1}$ (assuming a free carrier mobility value of $10 \text{ cm}^2/\text{V sec}$), and for a doping level of 10^{-3} , $E_a = 0.15$ eV, and $\sigma_0 = 21 \Omega^{-1}\text{cm}^{-1}$. Comparison with the data shows excellent agreement, with activation energies within 20 meV, and σ_0 within a factor of 4.

We next discuss the quantitative agreement with the data above the equilibration temperature. The known increase in N_{DB} (Ref. 14) causes E_{\min} to move towards E_C with increased doping level. From Fig. 3, it is seen that the model predicts activation energies ($E_a = E_C - E_{\min}$) of $E_a = 0.33$ eV for 1000 ppm PH_3 and $E_a = 0.37$ eV for 10

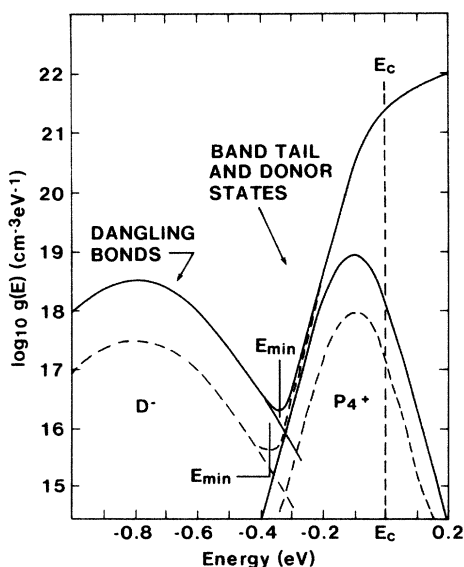


FIG. 3. A schematic diagram of the density of states showing the dangling-bond band and the band tail that includes the donor band for 10 ppm PH_3 (dashed line) and 1000 ppm PH_3 (solid line).

ppm PH_3 , within 50 meV of the measured data, which is well within the uncertainty of $g(E)$. Furthermore, the equivalent model for the valence band gives $E_a = 0.55$ eV for a doping of 10^{-3} , also in excellent agreement with the data. The larger activation energy in p -type material is due to the broader valence-band tail.

Finally, we address the conductivity prefactor in the high-temperature regime, where the statistical shift is absent. We estimate that the temperature dependence of the gap, $\exp(\gamma/k)$, gives a factor 1–2 in Eq. (4), assuming a uniform scaling of the gap energies. Therefore, the measured $\sigma_0 = 200 \Omega^{-1}\text{cm}^{-1}$, in the absence of a temperature dependence of E_C , yields

$$\sigma_{\min} \approx 100\text{--}200 \Omega^{-1}\text{cm}^{-1}. \quad (8)$$

For the p -type sample in Fig. 1, $\sigma_0 = 400 \Omega^{-1}\text{cm}^{-1}$ and $\exp(\gamma/k) \approx 2\text{--}4$, which gives the same σ_{\min} as Eq. (8). Our value for σ_{\min} is the same as that obtained by Overhof and Beyer⁴ after corrections for potential fluctuations, Fermi-level shifts, and electron-phonon couplings had been made.

The term σ_{\min} is the minimum metallic conductivity, first proposed by Mott,⁶ who calculated its value to be

$$\sigma_{\min} = 0.03e^2/\hbar a_E, \quad (9)$$

where a_E is the inelastic scattering length. Using the values for σ_{\min} in Eq. (8) gives

$$a_E = 3.5\text{--}7 \text{ \AA}, \quad (10)$$

a_E is the distance beyond which an electron will not, on average, maintain phase coherence; in the random-phase approximation (RPA) a_E is taken to be the spacing between adjacent sites at E_C .¹⁵ Mott's expression for a_E (Ref. 6) is

$$a_E/a = [N_C(E_m)/N_C(E_C)]^{1/3}, \quad (11)$$

where $N_C(E_C)$ is the density of states at E_C , $N_C(E_m)$ is the density of states at the middle of the conduction band, and a ($\approx 2.5 \text{ \AA}$) is the interatomic spacing. Inverse photoemission measurements by Jackson and co-workers¹⁶ have confirmed that near the conduction-band edge the RPA is valid. Using their results of $N_C(E_C) = 4 \times 10^{21} \text{ cm}^{-3}\text{eV}^{-1}$ and $N_C(E_m) = 3 \times 10^{22} \text{ cm}^{-3}\text{eV}^{-1}$ in Eq. (11) yields

$$a_E \approx 5 \text{ \AA}, \quad (12)$$

which agrees with the expected value. Moreover, the conductivity prefactor for transport above a well-defined mobility edge is given by³

$$\sigma_0 = N_C(E_C)kT\epsilon\mu_0, \quad (13)$$

where μ_0 is the microscopic mobility. Setting $\sigma_0 = \sigma_{\min}$ from Eq. (8), using the equilibration temperature for T , and setting $\mu_0 = 10 \text{ cm}^2/\text{V sec}$, we obtain

$$N_C(E_C) = (2\text{--}4) \times 10^{21} \text{ cm}^{-3}\text{eV}^{-1}, \quad (14)$$

in good agreement with the results of Jackson and co-workers. Thus there is full internal consistency between the measured prefactor, the density of states at E_C , and a free carrier mobility of $\sim 10 \text{ cm}^2/\text{V sec}$.

In summary, we have shown that the magnitude and temperature dependence of the dark conductivity of n -type doped a -Si:H can be completely explained by the defect-compensation model of doping when the defect structure is in metastable thermal equilibrium. We conclude with the following potentially controversial speculation. As shown in Figs. 1 and 2 there are two temperature regimes of σ , where both E_a and σ_0 are lower below the equilibration temperature than above it. An increase in σ_0 with E_a has been noted in conductivity measurements of a -Si:H (the Meyer-Neldel rule) and has been the source of much speculation.^{2,3} As shown here, for n -type doping the dif-

ferent values of σ_0 correspond to different physical processes; it would be misleading to plot σ_0 vs E_a for the data in Figs. 1 and 2. The Meyer-Neldel rule may be simply an artifact of comparisons of σ from differently doped and undoped a -Si:H samples. Clearly, further work needs to be done.

We are grateful to T. M. Hayes for helpful comments and the numerical computations, and to C. C. Tsai and R. Thompson for assistance in sample preparation. The research is supported by the Solar Energy Research Institute.

-
- ¹W. E. Spear and P. G. LeComber, *Solid State Commun.* **17**, 1193 (1975).
²H. Fritzsche and M. Tanielian, *AIP Conf. Proc.* **73**, 318 (1981).
³H. Fritzsche, *Sol. Energy Mater.* **3**, 447 (1980).
⁴H. Overhof and W. Beyer, *Philos. Mag. B* **47**, 377 (1983).
⁵D. A. Anderson and W. Paul, *Philos. Mag. B* **45**, 1 (1982).
⁶N. F. Mott, *Philos. Mag. B* **51**, 19 (1985); *Adv. Phys.* **34**, 329 (1985).
⁷R. A. Street, *Phys. Rev. Lett.* **49**, 1187 (1982).
⁸R. A. Street, J. Kakalios, and T. M. Hayes, *Phys. Rev. B* **34**, 3030 (1986).
⁹W. E. Spear, D. Allen, P. G. LeComber, and A. Ghaith, *J. Non-Cryst. Solids* **35 & 36**, 357 (1980).
¹⁰R. A. Street, J. C. Knights, and D. K. Biegelsen, *Phys. Rev. B* **18**, 1880 (1978).
¹¹M. Tanielian, *Philos. Mag. B* **45**, 435 (1982).
¹²D. L. Staebler and C. R. Wronski, *Appl. Phys. Lett.* **31**, 292 (1976).
¹³D. G. Ast and M. H. Brodsky, *Inst. Phys. Conf. Ser.* **43**, 1159 (1979).
¹⁴R. A. Street, *J. Non-Cryst. Solids* **77 & 78**, 1 (1985).
¹⁵Norman K. Hindley, *J. Non-Cryst. Solids* **5**, 17 (1970).
¹⁶W. B. Jackson, S. M. Kelso, C. C. Tsai, J. W. Allen, and S.-J. Oh, *Phys. Rev. B* **31**, 5187 (1985); W. B. Jackson, C. C. Tsai, and S. M. Kelso, *J. Non-Cryst. Solids* **77 & 78**, 281 (1985).